

1
2 **Probabilistic Fault Displacement Hazard Analysis for North Tabriz Fault**

3 Mohamadreza Hosseini¹, ~~Habib~~¹, Habib Rahimi, ²

4 *1. M.Sc. Graduated, Department of Earth Physics, Institute of Geophysics, University of Tehran, Tehran, Iran*

5 *2. Associate Professor, Department of Earth Physics, Institute of Geophysics, University of Tehran, Tehran, Iran*

6 *Corresponding author: Habib Rahimi; email: rahimih@ut.ac.ir*

Field Code Changed

7
8 **Abstract:**

9 The probabilistic fault displacement hazard analysis is one of the new methods ~~in~~^{of} estimating the amount of possible
10 displacement in the area at the hazard of causal fault rupture. In this study, using the probabilistic approach and
11 earthquake method introduced by Youngs et al., 2003, the surface displacement of the North Tabriz fault has been
12 investigated, and the possible displacement in different scenarios has been estimated. By considering the strike-slip
13 mechanism of the North Tabriz fault and using the earthquake method, the probability of displacement due to surface
14 ruptures caused by ~~the~~ 1721 and 1780 North Tabriz fault earthquakes has been explored. These events were associated
15 with 50 and 60 km of surface rupture, respectively. The 50-60 km long section of the North Tabriz fault was selected
16 as the source of possible surface rupture.

17 We considered two scenarios according to possible displacements, return periods, and magnitudes which are reported
18 in paleoseismic studies of the North Tabriz fault. ~~As~~^{In} the first scenario, possible displacement, return period, and
19 magnitude was selected between zero to 4.5; 645 years and Mw~7.7, respectively. In the second scenario, possible
20 displacement, return period and magnitude were selected between zero to 7.1, 300 years, and Mw~7.3, respectively.
21 For both mentioned scenarios, the probabilistic displacements for the rate of exceedance 5% in 50, 475, and 2475
22 years for the principle possible displacements (on fault) of the North Tabriz fault have been estimated. For the first
23 and second scenarios, the maximum probabilistic displacement of the North Tabriz fault at a rate of 5% in 50 years is
24 estimated to be 186 and 230 cm. Also, mentioned displacements for 5% exceedance in 475 years and 2475 years in
25 both return periods of 645 and 300 years, are estimated at 469 and 655cm.

26 **Keywords:** Surface rupture, Hazard, probabilistic fault displacement, North Tabriz fault, Iran.

27
28 Formatted: No bullets or numbering

29 **1- Introduction**

30 Earthquakes, not only because of earth-shaking but also because of surface ruptures, are a serious threat to
31 many human activities. Reducing earthquake losses and damages requires predicting the amplitude and location of
32 ground movements and possible surface displacements in the future. Fault displacement hazard assessments are based
33 on empirical relationships obtained using historical seismic rupture data. These relationships evaluate the probability

Formatted: Indent: First line: 0.5"

34 of co-seismic surface slip of ruptures on fault (primary) and outside the fault (distributed) for different magnitudes
35 and distances to the causal fault. In addition, these relationships make it possible to predict the extent of fault slip on
36 or near the active fault (Stephanie Baiz et al., 2019).

37 A way to reduce the effects of fault rupture hazards on a structure is to develop the probability of fault
38 displacement. This approach can be taken into account the rate of exceedance of different displacement levels of the
39 event under a structure, along with a displacement hazard curve (Youngs et al., 2003).
40 So far, fault displacement data have been collected and analyzed by several researchers to evaluate the fault rupture
41 So far, fault displacement data have been collected and analyzed by several researchers to
42 evaluate the fault rupture properties. Investigation of fault displacement and extraction of experimental relationships
43 are reported by Wells and Coppersmith (1993 and 1994) and reviewed by Petersen and Wesnousky (1994). To be
44 are reported by Wells and Coppersmith (1993 and 1994) and reviewed
45 by Petersen and Wesnousky (1994). To be considered, each earthquake causes a superficial shaking at the site, but
46 each earthquake does not cause a surface rupture in the area. Therefore, only the data of earthquakes that have caused
47 the rupture in the region are used to obtain the attenuation relationships (Youngs et al., 2003).

48 A method for estimating the probabilistic fault displacement hazard for strike-slip faults in the world has
49 been presented, mapped due to the impact of fault displacement hazard on the fault trace type and the complexity of
50 this effect and hazard of fault displacement for strike-slip faults studied (Petersen et al., 2011). Principal displacements
51 are considered primary ruptures that occur on or within a few meters of the active fault. Distributed displacements
52 outside the fault are causative and usually appear as discontinuous ruptures or shears distance several meters to several
53 hundred kilometers from the fault trace. The principal and distributed displacements are introduced as net
54 displacements derived from horizontal and vertical displacements (Petersen et al., 2011).

55 To estimate the probabilistic fault displacement hazard, we used the Petersen et al., 2011 method, but newly some
56 studies have been conducted in this approach. Recently,
57 Katona (2020) investigated the hazard of surface displacement due to faults in the design of nuclear power plants.
58 Katona (2020) investigated the hazard of surface displacement due to faults in the design of nuclear power plants.
59 Katona (2020) investigated the hazard of surface displacement due to faults in the design of
60 nuclear power plants. Nurminen et al. (2020) concentrate on off-fault rupturing and developed an original probability
61 model for the occurrence of distributed ruptures using 15 historical crustal earthquakes. Goda (2021) proposed an
62 alternative approach based on stochastic source modeling and fault displacement analysis using Okada equations. The
63 developed method is applied to the 1999 Hector Mine earthquake.

64 In this study, based on the results of a paleoseismic study reported by Hesami et al. (2003) on the North Tabriz fault,
65 the section with a length of 50 - 60 km was considered a source of possible rupture in the future. To describe the
66 possible behavior of the displacement rupture hazard of the North Tabriz fault, sites at distances of 50 m from each
67 other and cells with dimensions of 25 × 25 m² on fault trace were considered, which is shown in Figure 1. Also,
68 according to the study by Petersen et al. (2011), the trace of the North Tabriz fault was considered a simple trace
69 due to the absence of large instrumental earthquakes that are associated with surface rupture. Many studies have been

Formatted: Font color: Red

Formatted: Font color: Red

Formatted: Font color: Red

Formatted: Font color: Red

Formatted: Font color: Red

Formatted: Font color: Red

Formatted: Font color: Red

Formatted: Font color: Red

Formatted: Font color: Red

Formatted: Font color: Red

70 done on the historical displacements of the North Tabriz fault. According to the results of paleoseismic studies reported
71 by Hesami et al. (2003) and Ghasemi et al. (2015), the probabilistic displacement is between zero to 4.5 and zero to
72 7.1 m, respectively. The magnitude and return period of large earthquakes are considered 645 years with $M_w \sim 7.7$
73 and 300 years with $M_w \sim 7.3$ according to Mousavi et al. 2014 and Dejamour et al., 2011, respectively.

74 In the first step, probabilistic fault displacement and the annual rate of exceedance of displacement for
75 two given scenarios (645 years with $M_w \sim 7.7$) and (300 years with $M_w \sim 7.3$) have been achieved by considering 5%
76 in 50, 475, and 2475 years at the site with geographical coordinates (38.096, 46.349). In the second
77 step, due to the passage of the North Tabriz Fault through the city of Tabriz, considering a 2 km long section from the
78 North Tabriz Fault, the probabilistic displacement has been estimated, and the probabilistic displacement 2D map is
79 explored.

80

813-2- Seismotectonic

82 With over two million people and an area of 167 square kilometers in northwestern Iran, Tabriz is one of the
83 most populated cities in the country that has experienced devastating earthquakes throughout history. One of the main
84 problems of Tabriz City is the proximity of the city to the North Tabriz fault and the expansion of constructions around
85 it. Based on the reported historical earthquakes by Berberian and Arshadi (1979), since 858 AD., this city and the
86 surrounding area have experienced several large and medium destructive earthquakes.

87 The focal mechanism of earthquakes in northwestern Iran and southeastern Turkey shows that the convergence
88 between the Saudi and Eurasian plates becomes depreciable during right-lateral strike-slip faults. The strike-slip fault
89 is the southeastern continuation of the North Anatolian Fault into Iran, consisting of discontinuous fault sections with
90 a northwest-southeast extension (Jackson and Mackenzie et al., 1992). Some of these fault fragments have been
91 ruptured and left deformed along with the earthquakes in 1930, 1966, and 1976 (Hesami et al., 2003).

92 Nevertheless, the North Tabriz fault is one of the components of this right-lateral strike-slip system, which has not
93 had a major earthquake during the last two centuries. Among the many historical earthquakes in the Tabriz region,
94 only three devastating earthquakes with a magnitude of $M_s \sim 7.3$ in 1042, 1721, and 1780 with a magnitude of $M_s \sim 7.4$
95 had been associated with a surface rupture along the North Tabriz fault (Hesami et al., 2003). The 1721 and 1780 AD
96 earthquakes were along with at least 50 and 60 km of surface rupture (about 40 km overlap), respectively. Berberian
97 et al., 1997 believe that large earthquakes along the North Tabriz fault are concentrated at specific times and spatially
98 related.

99 The occurrence of the 1976 Chaldoran earthquake in Turkey, which was accompanied by about 55 km of fractures,
100 indicates that the length of the surface fracture caused by historical earthquakes in this region probably varies from
101 about 50 to 60 km (Toxos et al., 1977). A more detailed study of the temporal distribution of earthquakes in Tabriz by
102 Berberian and Yates (1999) also shows the cluster distribution of earthquakes over time. Due to the absence of seismic
103 events for more than 200 years in the Tabriz area (decluttering period), the study area has passed the final stages of

104 stress storage, and it is ready to release the stored energy. Therefore, Hesami et al., 2003 investigated the Spatial-
 105 temporal concentration of earthquakes associated with the North Tabriz fault. Based on paleontological seismic studies
 106 on the western part of the North Tabriz fault, Hesami et al., 2003 introduced four earthquakes that occurred
 107 continuously on the western part of the North Tabriz fault. The return periods of these earthquakes were suggested to
 108 be 821 ± 176 years. The amount of right-lateral strike-slip displacement, during each seismic event, of the North
 109 Tabriz fault, has been estimated at 3.5 to 4.5 m. In addition, Berberian et al., 1997 considered the possibility of
 110 fracturing all parts of the North Tabriz fault at once and mentioned it as one of the critical issues in the earthquake
 111 hazard for the Tabriz city and the northwestern region of Iran.

112
 113 In this study, the method introduced by Petersen et al., 2011 has been used to estimate the probabilistic fault
 114 displacement hazard caused by the North Tabriz fault. Details of the mentioned method are provided in Petersen et
 115 al., 2011, and a summary of this approach is provided here.

116 Probabilistic seismic hazard analysis has been used since its development in the late 1960s and early 1970s
 117 to assess shaking hazards and to establish seismic design parameters (Cornell, 1968 and 1971). A method for analyzing
 118 the hazard of probabilistic fault displacement was introduced in two approaches of earthquake and displacement
 119 (Youngs et al., 2003). This method was first proposed to estimate the displacement of Yucca Mountain faults, which
 120 were the landfill of nuclear waste (Stepp et al., 2001). Then, the probabilistic fault displacement hazard analysis
 121 method was introduced for an environment with normal faults, and the probability distributions obtained for each type
 122 of fault in the world can be used in areas with similar tectonics (Youngs et al., 2003).

123 The earthquake approach is similar to the analysis of probabilistic seismic hazard related to displacement, features
 124 such as faults, partial shear, fracture, or unbroken ground at or near the ground surface so that the attenuation
 125 relationships of the fault displacement replace the ground shaking relationships. In the displacement approach, without
 126 examining the rupture mechanism, the displacement characteristics of the fault observed at the site are used to
 127 determine the hazard in that area.

128 The exceedance rate of displacements and the distribution of fault displacements are obtained directly from
 129 the fault characteristics of geological features (Youngs et al., 2003). To calculate the rate of exceedance in the
 130 earthquake approach, similar to probabilistic seismic hazard analysis relationships were used. The rate of exceedance,
 131 $v_k(z)$, is calculated according to the Cornell relationship (1968 and 1971) as follows (Youngs et al., 2003):

$$132 \quad v_k(z) = \sum_n \alpha_n (m^0) \int_{m^0}^{m^H} f_n(m) \left[\int_0^\infty f_{kn}(r|m) \cdot P^*(Z > z|m, r) \cdot dr \right] \cdot dm \quad (1)$$

133 In which the ground motion parameter, (Z), (maximum ground acceleration, maximum response spectral acceleration)
 134 exceeds the specified level (z) at the site (k). Considering Equation (1) and ~~to calculate~~ calculating the exceedance rate
 135 of displacement (D) from a specific value (d), the displacement parameter replaces the parameters of ground motion
 136 (Youngs et al., 2003):

$$v_k(d) = \sum_n \alpha_n(m^0) \int_{m^0}^{m_n^0} f_n(m) \int_0^\infty f_{kn}(r|m) \cdot P^*(D > d|m, r) \cdot dr \cdot dm \quad (2)$$

137 The expression $P(D > d|m, r)$ is the "attenuation function" of the fault displacement at or near the earth's surface. This
 138 displacement attenuation function is different from the usual ground motion attenuation function and includes the
 139 multiplication of the following two probabilities (Youngs et al., 2003):

$$P_{kn}^*(D > d|m, r) = P_{kn}(\text{Slip}|m, r) \cdot P_{kn}(D > d|m, r, \text{slip}) \quad (3)$$

140 Which D and d are the Displacements on fault (principal fault) and displacement on the outside of the fault (distributed
 141 fault), **respectively-respectively** (x, y) are considered as coordinates of the site. $r, z^2, I, L,$ and s are the vertical distance
 142 from the fault, area, the distance of site on fault rupture to the nearest rupture, the total length of the fault surface
 143 rupture, and the rupture distance to the end of the fault, respectively. The definition of these variables is shown in
 144 figure (2).

145 The following Equation has been used to obtain the exceedance rate of probabilistic displacement due to the principal
 146 fault (on fault) (Petersen et al., 2011):

$$\lambda(D \geq D_0)xyz = \alpha(m) \int_{m,s} f_{M,S}(m, s) P[SR \neq 0|m] * \int_r P[D \neq 0|z, sr \neq 0] * P[D \geq D_0 | L, m, D \neq 0] f_R(r) dr dmds \quad (4)$$

147 The magnitude of the earthquake is indicated by m . In relation 4 and to assess the displacement hazard due to fault
 148 rupture, the probability density functions that describe displacement potential due to earthquakes on or near a rupture,
 149 as well as the probabilities that the potential for non-zero ruptures are used (Petersen et al., 2011). In the following,
 150 each of the parameters for estimation of probabilistic fault displacement hazard is described.

151 3-1 Probability density function

152 The probability density function $f_{M,S}(m, s)$ determines the magnitude of the earthquake and the location of
 153 the ruptures on a fault. Since the magnitude and the rupture position on the causal fault are correlated, a probabilistic
 154 distribution is used to calculate these parameters. In the next step, the variability in the rupture location is considered.
 155 A probability density function $f_R(r)$ is considered to define the area of perpendicular distances (r) to the site to different
 156 potential ruptures (Petersen et al., 2011).

157 3-2 Probabilities

158 Probability $P[SR \neq 0 | M]$ is the ratio of cells with rupture on the principal fault to the total number of cells
 159 considered. Therefore, the probability of surface rupture $P[SR \neq 0 | M]$ is considered due to a certain magnitude M
 160 due to faulting. According to studies **of-by** Wells and Coppersmith (1993), due to the formulation of empirical
 161 relationships between different fault parameters, probability has been obtained for different faults in the world, such
 162 as strike-slip, normal, and revers. Therefore, in hazard analysis of fault displacement, it is necessary to investigate the

163 possibility of surface rupture with magnitude (M) on the ground so as a result, the equation (5) introduced by Wells
 164 and Coppersmith (1993) can be used. According to this relation, the coefficients a and b are constant, and strike-slip
 165 faults with -12.51 and 2.553 have been reported. This relationship has a 10% probability for the size of Mw~5 and a
 166 95% probability of surface rupture for a magnitude of Mw~7.5 ((Rizzo et al., 2011).

167

$$P[sr \neq 0|m] = \frac{e^{a+bm}}{1+e^{a+bm}} \quad (5)$$

168 This rupture probability was used to estimate the exceedance rate of displacement because of earthquakes such as
 169 Loma-Prieta in 1989 with a magnitude of Mw~6.9 and Alaska in 2002 with a magnitude of Mw~6.7. These
 170 earthquakes did not cause rupture to reach the earth's surface. Therefore, these two earthquakes did not cause surface
 171 deformation and are considered non-tectonic phenomena (Petersen et al., 2011). The expression $P[D \neq 0|z, sr \neq 0]$
 172 indicates the probability of non-zero displacement at a distance r from the rupture in an area of size z^2 and due to the
 173 magnitude event m associated with the surface rupture. The probability $P[D \geq D_0|L, m, D \neq 0]$ for displacements
 174 more significant than or equal to the value given at this site is intended for the principal displacement (on fault). This
 175 probability is obtained by integrating around a log-normal distribution (Petersen et al., 2011).

176

177 **3-3 Rate parameter $\alpha(m)$:**

178 When the potential magnitude of an earthquake with a certain magnitude is modeled, it is possible to estimate how
 179 often these ruptures occur. The, $\alpha(m)$, rate parameter used describes the frequency of repetition of these earthquakes
 180 in this model. This parameter is a function of magnitude and can only function as a single rupture function or a function
 181 of cumulative earthquakes above the magnitude of the minimum importance in engineering projects (Youngs et al.,
 182 2003). This parameter is usually based on slip rate, paleoseismic rate of large earthquakes, or historical fault rate
 183 earthquakes and is described in earthquake units per year. By removing the $\alpha(m)$ parameter from Equation (4), the
 184 Deterministic Fault Displacement Hazard can be estimated (Petersen et al., 2011).

185

186 **3-4 Cell size:**

187 In calculating the hazard of principal fault displacements, as shown in Eq. (4), by changing the size of the cells, the
 188 level of hazard will not change and this parameter can be examined by the availability of principal displacement data
 189 in the study area. In calculating the hazard of distributed rupture (distributed displacement), considering the method
 190 of Youngs et al. (2003), by modeling secondary displacements up to a distance of 12 km from the fault, the probability
 191 of surface rupture was investigated. According to studies by Petersen (2011), the relationship between the calculations
 192 of the probability of rupture of the principal faults (5), in calculating the probability of rupture of the distributed faults
 193 became the following relationship (Petersen et al., 2011):

194

$$\ln(p) = a(z) \ln(r) + b(z) \quad (6)$$

195 The values of the coefficients used for the cell sizes of 25x25 to 200x200 m² in the above relationship are given in
 196 Table 1 (Petersen et al., 2011).

197

198 **3-5 Surveying accuracy**

199 The accuracy of fault location is a function of geological and geomorphic conditions that play an essential
200 role in diagnosing and interpreting a geologist in converting this spatial information into geological maps and fault
201 geographic information systems. A fault map is generated using aerial photography imagery, interpretation of fault
202 patterns from geomorphology, and conversion of fault locations into a base map. In many cases, identifying the
203 location and trace of the fault may be difficult because sediments and erosion may obscure or cover the fault surface,
204 leading to more uncertainty in identifying the actual location of the fault. Therefore, trace mapped faults are divided
205 into four categories: accurate, approximate, inferred, and concealed, based on how clearly and precisely they are
206 located (Petersen et al., 2011).

207 A practical example shows that an active fault with large earthquakes repeated over several hundred years, fault
208 rupture hazard analysis should be one of the critical topics considered for the design of structures or pipelines that are
209 close to this fault, and if the fault has a complex or straightforward trace, avoiding the fault from the constructo
210 to a distance of 150 and 300 meters, respectively. Table 2 summarizes the standard deviations for the displacements
211 observed in strike-slip earthquakes for different classifications of mapping accuracy (Petersen et al., 2011). According
212 to the exponential values obtained from these fitting equations, the mean displacement will be obtained. The following
213 Equation has been used to obtain the mean displacement (Petersen et al., 2011):

$$D_{mean} = e^{\mu + \sigma^2/2} \quad (7)$$

214

215

216 **3-6 Epistemic and Aleatory uncertainty**

217 There are uncertainties about the quality of mapping and the complexity of the fault trace that lead to epistemic
218 uncertainty at the site of future faults. The probability density function for r includes both epistemic and aleatory
219 components. Displacements on and off the principal fault can include components of epistemic uncertainty and
220 random variability. Epistemic uncertainty is related to displacement measurement errors along fault rupture. Random
221 variability is related to the natural variability in fault displacements between earthquakes. However, the measured
222 variability in ruptures involves epistemic mapping uncertainties because there is currently no data to separate these
223 uncertainties. In addition, epistemic uncertainty of location is introduced due to limitations in the accuracy of basic
224 maps or images and the accuracy of the equipment used to transfer this information to the map or database (Petersen
225 et al., 2011).

226 **3-7 Attenuation relationship of strike-slip faults**

227 In this study, to estimate the probabilistic displacement of the North Tabriz fault, the attenuation relationship of
228 Petersen et al. (2011) has been used. The rupture displacement data obtained from the principal fault are scattered but
229 are generally the most scattered near the fault rupture center and decrease rapidly at the end of the rupture. In some
230 earthquakes, including the Borgo Mountain earthquake in 1968, the most significant displacement was observed near

231 the end of the fault surface rupture (Petersen et al., 2011). Many of the collected surface rupture data behave
232 asymmetrically ruptured (Wesnousky et al., 2008). However, there is currently no way to determine surface rupture
233 areas that have larger displacements. Thus, the distribution of asymmetric displacements along the length of a fault
234 will define more considerable uncertainties, especially near the end of the fault rupture (Petersen et al., 2011). To
235 determine the displacement distribution, and the principal fault, two different approaches were introduced by Petersen
236 et al. (2011). In the first approach, the best-fit equations using the least-squares method related to the natural logarithm
237 of the displacement ratio of magnitude and distance were developed in a multivariate analysis (Paul Rizzo et al., 2013).
238 In the second approach, the displacement data is normalized by the average displacement as a distance function. In
239 normalized analysis, magnitude is not directly considered but influences calculations through the presence of
240 magnitude in the mean displacement, which is calculated through the studies of Wells and Coppersmith (1994). Three
241 models (bilinear, elliptical and quadratic) were considered to provide the principal fault displacement in multivariate
242 and normalized analysis (Petersen et al., 2011). However, in multivariate analysis, the three introduced models have
243 the same aleatory uncertainty, and there is no clear basis for preferring one model to the other models. As a result, in
244 the probabilistic displacement hazard analysis, all three models with the same weights were used according to Table
245 3. The results obtained from the multivariate analysis were preferred over the normalized analysis because, in the
246 normalized analysis, the stochastic uncertainty of calculating the mean displacement from the Wells and Coppersmith
247 (1994) study is added to the stochastic uncertainty of the results of the Petersen attenuation relationships (Paul Rizzo
248 et al., 2013).

249
250 In this study, multivariate analysis and probabilistic displacement estimation have been used in the three mentioned
251 models. The Equation of the three models is obtained in the multivariate method as shown in Table 3, and 5%
252 uncertainty was considered in the modeling of the strike-slip displacement data (Petersen et al., 2011):

254 4 Results and Discussions

255 In this study, we assumed the North Tabriz fault as a simple trace with the strike-slip focal mechanism. Due to the
256 lack of instrumental data on surface ruptures, two scenarios (Mw~7.7, 645years), and (Mw~7.3, 300years) was
257 considered a probabilistic surface rupture in the future. The length of the fault section was considered 50- 60 km and
258 the probabilistic displacement, and the annual exceedance rate was estimated by considering one of the sites located
259 on the Tabriz fault trace related to the total segment as shown in Figure 1. In addition, for each scenario, two values
260 of displacement (zero to 4.5m) and (zero to 7.1m) were considered according to Hessami et al., 2003 and Ghassemi
261 et al., 2015, respectively. Furthermore, considering the reported method by Petersen et al., 2011, the probabilistic
262 displacements for an exceedance rate of 5% in 50, 475, and 2475 years for the principal probabilistic displacements
263 (on fault) of the North Tabriz fault have been explored. The obtained results in this study can be summarized as
264 follows.

265 By considering the reported 4.5 m probable surface displacement by Hessami et al., 2003, maximum displacement for
266 the first scenario (Mw~7.7, 645years) and 5% in 50, 475, and 2475years were estimated at 186, 469, and 469 cm. For

Formatted: Not Highlight

267 the second scenario ($M_w \sim 7.3$, 300years), the maximum displacement was calculated at 230, 469, and 469cm,
268 respectively as shown in figure (3a). In addition, by considering the 7.1m probable surface displacement reported by
269 Ghassemi et al., 2015, maximum displacement for the first scenario of ($M_w \sim 7.7$, 645years) and 5% in 50, 475, and
270 2475years was estimated at 186, 655, and 655cm. For the second scenario ($M_w \sim 7.3$, 300years), the maximum
271 displacement was calculated at 230, 655, and 655 cm, respectively which is shown in figure (3b).

272 According to the results shown in Figures 3a and 3b, although in some cases and distances, the estimated maximum
273 displacement values are the same, at farther distances perpendicular to the site, these values are different from each
274 other.

275 For both scenarios ($M_w \sim 7.7$, 645 years and $M_w \sim 7.3$, 300 years), taking into account the maximum possible
276 displacements reported from other studies (0 to 4.5m and 7.1m), the maximum displacements for 5% in 475years were
277 observed up to a distance of 60 meters perpendicular to the assumed site.

278 For the first scenario ($M_w \sim 7.7$, 645 years), the maximum displacement for 5% in 2475 years using probable
279 displacements 0 to 4.5m and 0 to 7.1 m were calculated up to 100m and 80m perpendicular to the assumed site,
280 respectively. For the second scenario ($M_w \sim 7.3$, 300 years), the maximum displacement for 5% in 2475 years using
281 probable displacement of 0 to 4.5m and 0 to 7.1 m were observed up to 80m and 40m perpendicular to the assumed
282 site, respectively.

283 As mentioned, the fitting models (bilinear, elliptical, and quadratic) have similar uncertainties, and in this section, we
284 compared the estimated displacements obtained by using these models. In this study, the bilinear model is used to
285 obtain probabilistic displacements. The values of the probabilistic displacements were obtained for the mentioned
286 models. In figure 4, estimated probability displacement has been compared using different fitting models.

287 In the next step, for both scenarios of 4.5 and 7.1m displacements, the annual rate of exceedance of displacement (5%
288 in 50 years), at distances 64 and 120m from the assumed site, has been examined and shown in figure 5. For both
289 scenarios, $M_w \sim 7.7$, 645 years and $M_w \sim 7.7$, 645 years, the results are shown in Figures 5 a and b.

290 Concerning a part of the North Tabriz fault that passes through the 15th district of Tabriz city, estimating the
291 probabilistic displacement in this area is of great importance, and predicting the areas with a higher level of surface
292 rupture hazard is an important matter.

293 Considering a cross-section with a length of 2 km from the North Tabriz fault according to Figures (6, 7, and 8), the
294 possible two-dimensional displacements for the North Tabriz fault have been estimated. To estimate the probabilistic
295 displacement, two scenarios ($M_w \sim 7.7$, 645years) and ($M_w \sim 7.3$, 300years) were considered. Figure (6) shows the
296 probabilistic displacement of the two mentioned scenarios for the 5% in 50 years. The probabilistic displacements for
297 the 4.5 and 7.1m displacements for the first scenario are shown in Figures 6a and 6b, respectively. For the second
298 scenario, those results are shown in Figures 6c and 6d.

299 For the second scenario, the probabilistic displacement values have a higher level of hazard that can be seen at greater
300 distances from the assumed sites. The probabilistic displacement of the two scenarios for the 5% in 475 and 2475

Formatted: Not Highlight

Formatted: Not Highlight

301 years are shown in Figures 7 and 8, respectively. The values of displacement perpendicular to the assumed site and
302 the amount of probability hazard in the area were investigated and illustrated in Figure (9), and the two scenarios
303 ($M_w \sim 7.7$, 645years) and ($M_w \sim 7.3$, 300years) were compared. According to Figure 9a for 5% in 50years, the scenario
304 ($M_w \sim 7.3$, 300years) has a higher level of hazard and can be considered the worst-case scenario. The numerical value
305 of the displacement is obtained equally in the two displacement cases (4.5 and 7.1m). The first scenario, given that it
306 has a larger magnitude than the second scenario ($\Delta m = 0.4$), but due to the higher return period, has a lower level of
307 risk than the second scenario. In the case of 5% in 475years and 2475years, according to Figures (9b and 9c), unlike
308 the case of 50years, the first scenario has a higher level of hazard and is more important, and can be considered as the
309 worst-case scenario.

310 5 Conclusion

311 Assuming the North Tabriz fault as a simple trace with a strike-slip focal mechanism
312 , and considering two scenarios ($M_w \sim 7.7$, 645yrs), and ($M_w \sim 7.3$, 300yrs) and a
313 fault section with a length of 50 - 60 km, the probabilistic displacement of the North Tabriz fault was estimated.
314 Furthermore, considering the reported approach by Petersen (2011), the probabilistic displacements for an exceedance
315 rate of 5% in 50, 475, and 2475 years for the principal probabilistic displacements (on fault) of the North Tabriz fault
316 have been explored. The obtained results in this study can be summarized as follows.

- 317 1- We considered two scenarios according to possible displacements, return periods, and magnitudes which are
318 reported in paleoseismic studies of the North Tabriz fault.
- 319 2- In the first scenario, possible displacement, return period and magnitude were selected between zero to 4.5;
320 645 years and $M_w \sim 7.7$, respectively. In the second scenario, possible displacement, return period and
321 magnitude were selected between zero to 7.1, 300 years, and $M_w \sim 7.3$, respectively.
- 322 3- For both above-mentioned scenarios, the probabilistic displacements for the rate of exceedance 5% in 50,
323 475, and 2475 years for the principle possible displacements (on fault) of the North Tabriz fault have been
324 estimated. For the first and second scenarios, the maximum probabilistic displacement of the North Tabriz
325 fault at a rate of 5% in 50 years is estimated to be 186 and 230 cm.
- 326 4- Maximum displacements for 5% exceedance in 475 years and 2475 years in both return periods of 645 and
327 300 years are estimated at 469 and 655cm.
- 328 5- In this study, the probability displacement values of the North Tabriz fault have been obtained without
329 considering the dip, depth, and rake of the fault, which has caused the same displacement values in the north
330 and south plane of the fault. In future studies, it is possible to investigate the geometric properties of the
331 source producing surface rupture and reduce the recognition uncertainty in the method of probabilistic fault
332 displacement hazard analysis.
- 333 6- The lack of large instrumental earthquakes in northwestern Iran leads to more significant epistemic
334 uncertainty in the obtained values. Due to the passing of the North Tabriz fault through the residential area
335 of Tabriz and destructive historical earthquakes, it is crucial to estimate the possible future displacements of
336 this fault.

337

338 **Conflicts of interests**

339 The authors declare that they have no known competing financial interests or personal relationships that
340 could have appeared to influence the work reported in this paper.

341

342 **References**

- 343 Ambraseys, N.N., and Melville, C.P.: A History of Persian Earthquakes, Cambridge University Press,
344 England, 236, 1982.
- 345 Barka, A.: the 17 August 1999 Izmit Earthquake, *Science.*, 285, 5435, 1858–1859,
346 doi:10.1126/science.285.5435.1858, 1999.
- 347 Baize, S., Nurminen, F., Dawson, T., Takao, M., Azuma, T., Boncio, P., Marti, E.: A Worldwide and
348 Unified Database of Surface Ruptures (SURE) for Fault Displacement Hazard Analyses, *Bull. Seismol. Soc. Am.*,
349 499-520, <https://doi.org/10.1785/0220190144>, 2019.
- 350 Berberian, M.: Patterns of historical earthquake rupture on the Iranian plateau. In *Developments in Earth*
351 *Surface Processes*, 17, <https://doi.org/10.1016/B978-0-444-63292-0.00016-8>, 2014.
- 352 Berberian, M., & Yeats, R. S.: Patterns of historical earthquake rupture in the Iranian Plateau, *Bull.*
353 *Seismol. Soc. Am.*, 89, 1, 120-139, 1999.
- 354 Berberian, M.: Seismic Sources of the Transcaucasian Historical Earthquakes, *Nato. Asi. 2.*, 233–311.
355 https://doi.org/10.1007/978-94-011-5464-2_13, 1997.
- 356 Berberian, M., and Arshadi, S.: On the evidence of the youngest activity of the North Tabriz Fault and the
357 seismicity of Tabriz city, *Geol. Surv. Iran Rep.*, 39, 397–418, 1976.
- 358 Biasi, G. P., and Weldon, R. J.: Estimating surface rupture length and magnitude of paleoearthquakes from
359 point measurements of rupture displacement, *Bull. Seismol. Soc. Am.*, 96, 1612–1623, 2006.
- 360 Bouchon, M., Bouin, M. P., Karabulut, H., Toksöz, M. N., Dietrich, M., Rosakis, A. J.: How Fast is
361 Rupture during an Earthquake? New Insights from the 1999 Turkey Earthquakes, *Geophys. Res. Lett.*, 28, 14, 2723–
362 2726, 2001.
- 363 Comfort, L.: Self-Organization in Disaster Response: The Great Hanshin Earthquake of January 17, 1995,
364 *Nat. Hazards.*, 12, 1995.
- 365 Coppersmith, K. J., & Youngs, R. R.: Data needs for probabilistic fault displacement hazard analysis, *J.*
366 *Geodyn.*, 29, 329–343, [https://doi.org/10.1016/S0264-3707\(99\)00047-2](https://doi.org/10.1016/S0264-3707(99)00047-2), 2000.
- 367 Cornell, C. A.: Engineering seismic risk analysis, *Bull. Seismol. Soc. Am.*, 58, 5, 1583–1606,
368 <https://doi.org/10.1785/BSSA0580051583>, 1968.
- 369 Djamour, Y., Vernant, P., Nankali, H. R., Tavakoli, F.: NW Iran-eastern Turkey present-day kinematics:
370 Results from the Iranian permanent GPS network, *Earth. Planet. Sc. Lett.*, 307, 1–2, 27–34,
371 <https://doi.org/10.1016/j.epsl.2011.04.029>, 2011.
- 372 Ghassemi, M. R.: Surface ruptures of the Iranian earthquakes 1900-2014: Insights for earthquake fault
373 rupture hazards and empirical relationships, *Earth-Sci. Rev.*, 156, 1–13,
374 <https://doi.org/10.1016/j.earscirev.2016.03.001>, 2016.

375 Hemphill-Haley, M. A., and Weldon II R. J.: Estimating prehistoric earthquake magnitude from point
376 measurements of surface rupture, *Bull. Seismol. Soc. Am.*, 89, 1264–1279,
377 <https://doi.org/10.1785/BSSA0890051264>, 1999.

378 Hessami, K., Pantosti, D., Tabassi, H., Shabani, E., Abbassi, M. R., Fegghi, K., & Solaymani, S.:
379 Paleoearthquakes and slip rates of the North Tabriz Fault, NW Iran: Preliminary results, *Ann. Geophys-Italy.*, 46, 5,
380 903–916, <https://doi.org/10.4401/ag-3461>, 2003.

381 Jennings, P. C.: Engineering features of the San Fernando earthquake of February 9, 1971, California
382 Institute of Technology, (Unpublished), <https://resolver.caltech.edu/CaltechEERL:1971.EERL-71-02>, 1971.

383 Koketsu, K., Yoshida, Sh., Higashihara, H.: A fault model of the 1995 Kobe earthquake derived from the
384 GPS data on the Akashi Kaikyo Bridge and other datasets, *Earth. Planets. Sp.*, 50, 10, 803,
385 <https://doi.org/10.1186/BF03352173>, 1998.

386 Lee J. C., Chu H. T., Angelier, J., Chan Y.C., Hu J.C., Lu C.Y., Rau R.J.: Geometry and structure of
387 northern surface ruptures of the 1999 Mw=7.6 Chi-Chi Taiwan earthquake: influence from inherited fold belt
388 structures: *J. Struct. Geol.*, 24, 1, 173–192, [https://doi.org/10.1016/S0191-8141\(01\)00056-6](https://doi.org/10.1016/S0191-8141(01)00056-6), 2002.

389 Masson, F., Djamour, Y., Van Gorp, S., Chéry, J., Tatar, M., Tavakoli, F., Vernant, P.: Extension in NW
390 Iran driven by the motion of the South Caspian Basin, *Earth. Planet. Sc. Lett.*, 252, 1–2, 180–188,
391 <https://doi.org/10.1016/j.epsl.2006.09.038>, 2006.

392 Mirzaei, N., Gao, M. and Chen, Y. T.: Seismic source regionalization for seismic zoning of Iran: Major
393 Seismotectonic provinces, *J. Earthquake. Pred. Res.*, 7, 465–495, 1998.

394 Moss, R. E. S., & Ross, Z. E.: 2011, Probabilistic fault displacement hazard analysis for reverse faults,
395 *Bull. Seismol. Soc. Am.*, 101, 4, 1542–1553, <https://doi.org/10.1785/0120100248>, 2011.

396 Mousavi-Bafrouei, S. H., Mirzaei, N., and Shabani, E.: A declustered earthquake catalog for Iranian
397 plateau, *Ann. Geophys-Italy.*, 57, 6, <https://doi.org/10.4401/ag-6395>, 2014.

398 Paul C., Rizzo Associates, I.: Probabilistic Fault Displacement Hazard Analysis Krško East and West Sites
399 Proposed Krško 2 Nuclear Power Technical Report Probabilistic Fault Displacement Hazard Analysis Krško East
400 and West Sites Proposed Krško 2 Nuclear Power Plant, 2013.

401 Petersen, M. D., and Wesnousky, S. G.: Fault slip rates and earthquake histories for active faults in
402 southern California, *Bull. Seismol. Soc. Am.*, 84, 1608–1649, <https://doi.org/10.1785/BSSA0840051608>, 1994.

403 Petersen, M. D., Dawson, T. E., Chen, R., Cao, T., Wills, C. J., Schwartz, D. P., & Frankel, A. D.: Fault
404 displacement hazard for strike-slip faults, *Bull. Seismol. Soc. Am.*, 101, 2, 805–825,
405 <https://doi.org/10.1785/0120100035>, 2011.

406 Ram, T. D., & Wang, G.: Probabilistic seismic hazard analysis in Nepal: *Earthq. Eng. Eng. Vib.*, 12, 4,
407 577–586, <https://doi.org/10.1007/s11803-013-0191-z>, 2013.

408 Rui, Ch., Petersen, M. D.: Improved Implementation of Rupture Location Uncertainty in Fault
409 Displacement Hazard Assessment, *Bull. Seismol. Soc. Am.*, 109, 5, 2132–2137.
410 <https://doi.org/10.1785/0120180305>, 2019.

411 Shahvar, M. P., Zare, M., and Castellaro, S.: A unified seismic catalog for the Iranian plateau (1900–
412 2011), *Seismol. Res. Lett.*, 84, 233–249, 2013.

413 Stepp, J. C., Wong, I., Whitney, J., Quittmeyer, R., Abrahamson, N., Toro, G., Sullivan, T.: Probabilistic
414 seismic hazard analyses for ground motions and fault displacement at Yucca Mountain, Nevada: *Earthq. Spectra.*,
415 17, 1, 113–151. <https://doi.org/10.1193/1.1586169>, 2001.

416 Toksöz, M. N., ARPAT, E., & ŞARO&GLU, F. U. A. T.: The East Anatolian earthquake of 24 November
417 1976, *Nature.*, 270(5636), 423-425, <https://doi.org/10.1038/270423b0>, 1977.

418 Wells, D. L., & Coppersmith, K. J.: New Empirical Relationships among Magnitude, Rupture Length,
419 Rupture Width, Rupture Area, and Surface Displacement, *Bull. Seismol. Soc. Am.*, 84, 4, 974-1002,
420 <https://doi.org/10.1785/BSSA0840040974>, 1994.

421 Wells, D. L., & Kulkarni, V. S.: Probabilistic fault displacement hazard analysis - Sensitivity analyses and
422 recommended practices for developing design fault displacements, NCEE 2014 - 10th U.S. National Conference on
423 Earthquake Engineering: Frontiers of Earthquake Engineering, October 2014, <https://doi.org/10.4231/D3599Z26K>,
424 2014.

425 Wesnousky, S. G.: Displacement and geometrical characteristics of earthquake surface ruptures: Issues and
426 implications for seismic-hazard analysis and the process of earthquake rupture, *Bull. Seismol. Soc. Am.*, 98, 4,
427 1609-1632. <https://doi.org/10.1785/0120070111>, 2008.

428 Young, C. J., Lay, T., & Lynnes, C. S.: Rupture of the 4 February 1976 Guatemalan earthquake: *Bull.*
429 *Seismol. Soc. Am.*, 79, 3, 670-689, <https://doi.org/10.1785/BSSA0790030670>, 1989.

430 Youngs, R. R., Arabasz, W. J., Anderson, R. E., Ramelli, A. R., Ake, J. P., Slemmons, D. B., Toro, G. R.:
431 A methodology for probabilistic fault displacement hazard analysis (PFDHA), *Earthq. Spectra.*, 19, 1, 191-219.
432 <https://doi.org/10.1193/1.1542891>, 2003.

433

434

435

436

437

438

439

440

441

442

443

444

445

446

447

448

449

450

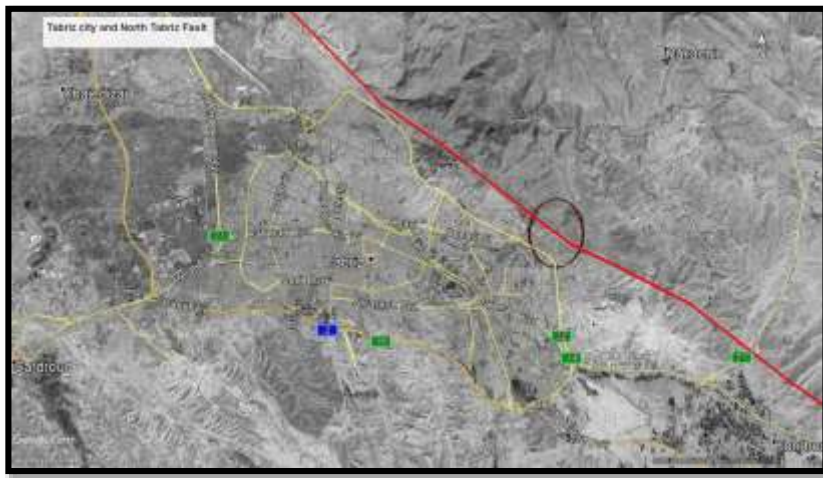
451

452

453

454

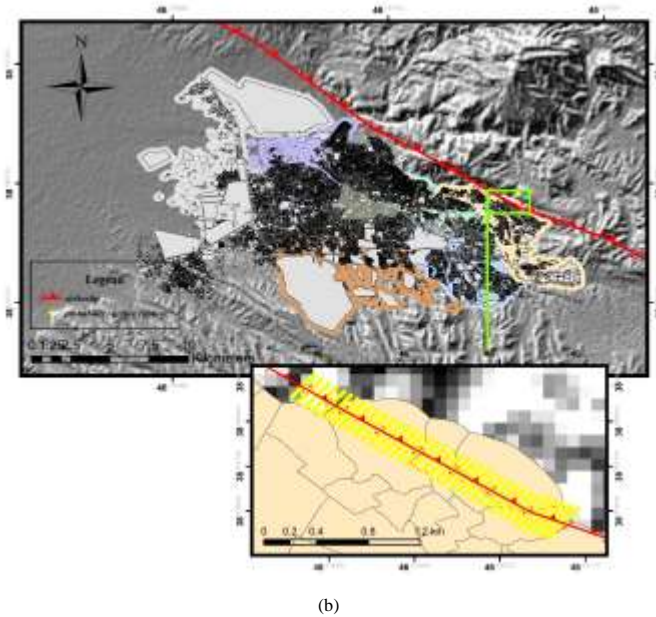
List of figures:



455

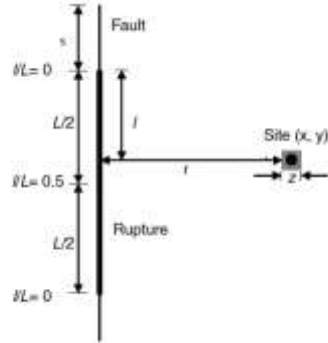
456

(a)



457
458

459 Figure 1. North Tabriz Fault and Tabriz city (a), Part of the North Tabriz fault considered in this study, and perpendicular
460 profiles (b). Figure a and b are generated using Google Earth with Digital Globe imagery (© Google Earth 2021).

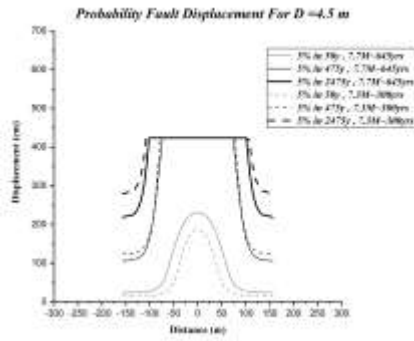


461

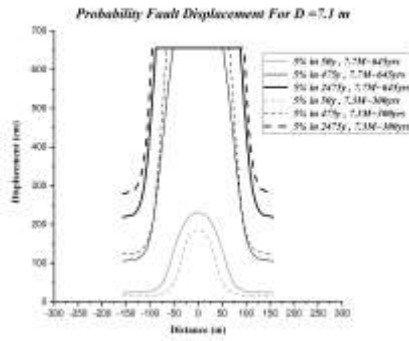
462 Figure 2. Definition of the variables used in fault rupture analysis: x and y Site coordinates, z Dimensions of the area intended to calculate the
463 probability of fault rupture at the site (for example, dimensions of the building foundation), r : the distance from the site to the fault trace, ratio l/L
464 l : the distance from the fault so that l is the measured distance from the nearest point on the rupture to the nearest end of the rupture, L : the total
465 length of the rupture and s : the distance from the end of the rupture to the end of the fault (Petersen et al., 2011).

466

467



(a)



(b)

468

469

Figure 3. Comparison of probability displacement, 5% exceedance rate in 50, 475, and 2475 years for a) D=4.5 m b) D=7.1 m

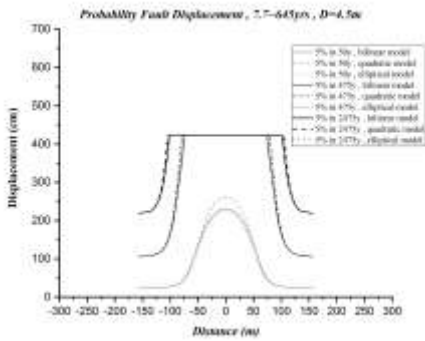
470

471

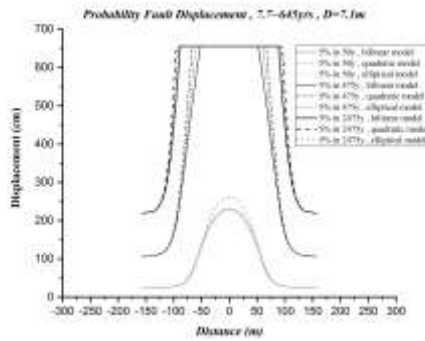
472

473

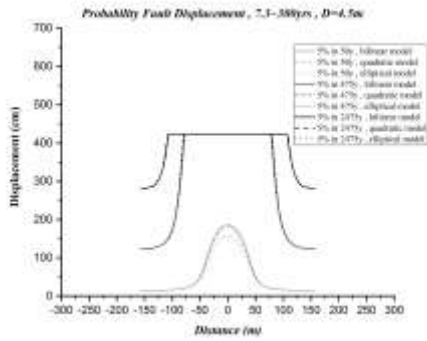
474



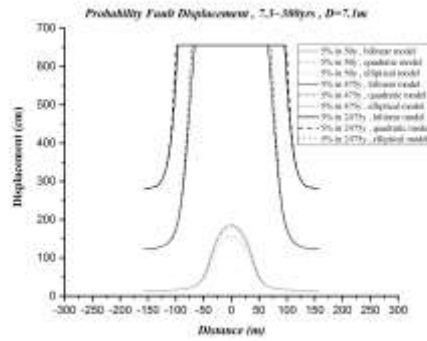
(a)



(b)



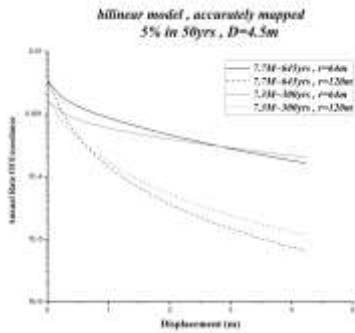
(c)



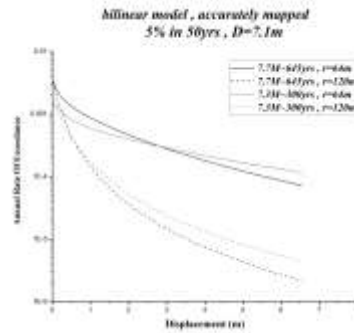
(d)

475 Figure 4. Comparison of probability displacement, different fitting models for a) 645-year return period and D=4.5 m, b) 645-year return period
476 and D= 7.1m, c) 300-year return period and 4.5 m, d) return period 300- years, and D=7.1 m

477
478
479
480
481



(a)

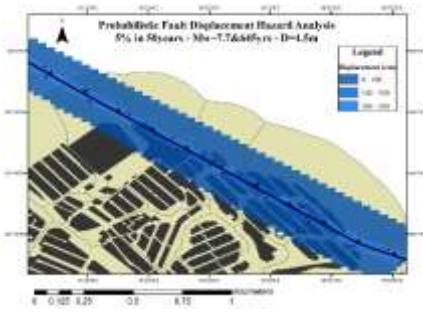


(b)

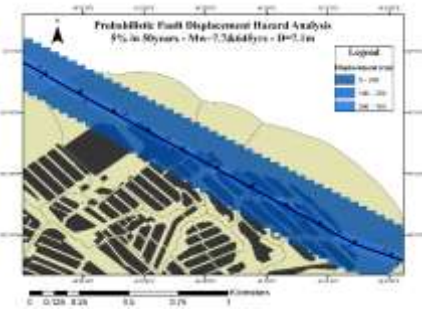
482 Figure 5. Comparison of the annual rate of exceedance of displacement for a) D=4.5 m displacement, b) D=7.1 m displacement

483
484

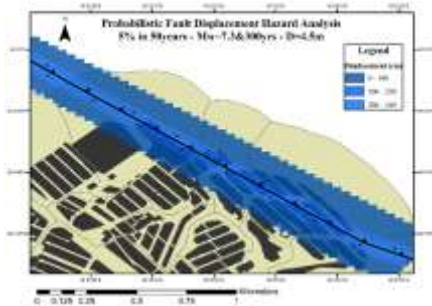
485
486
487
488
489
490
491
492
493
494
495
496
497
498
499
500



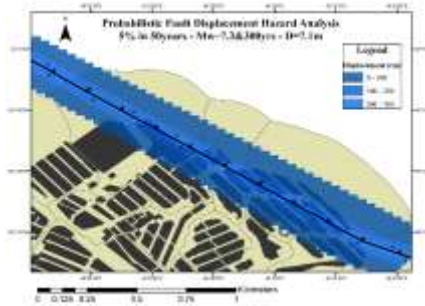
(a)



(b)



(c)



(d)

501

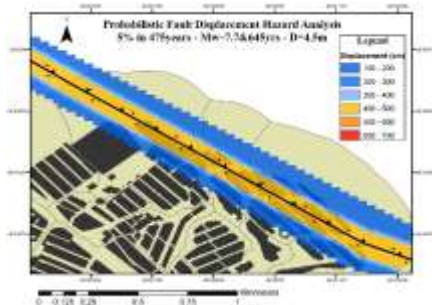
502 Figure 6. Probability Displacement of 5% in 50, a) Mw~7.7 and return period of 645yrs for D=4.5m, b) Mw~7.7 and return period of 645yrs for
503 D=7.1m, c) Mw~7.3 and return period of 300yrs for D=4.5m and d) Mw~7.3 and return period of 300yrs for D=7.1m

504

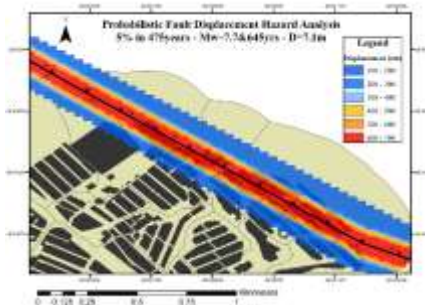
505

506

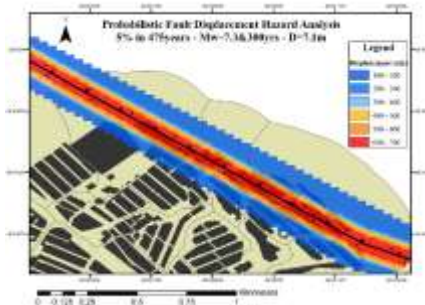
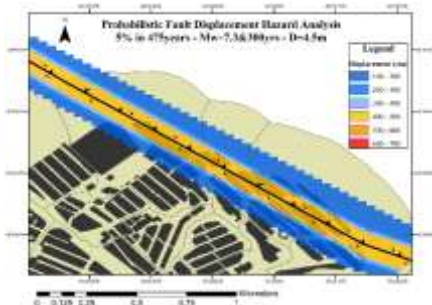
507



(a)



(b)



(c)

(d)

508

509 Figure 7. Probability Displacement of 5% in 475, a) Mw~7.7 and return period of 645yrs for D=4.5m, b) Mw~7.7 and return period of 645yrs for
510 D=7.1m, c) Mw~7.3 and return period of 300yrs for D=4.5m and d) Mw~7.3 and return period of 300yrs for D=7.1m

511

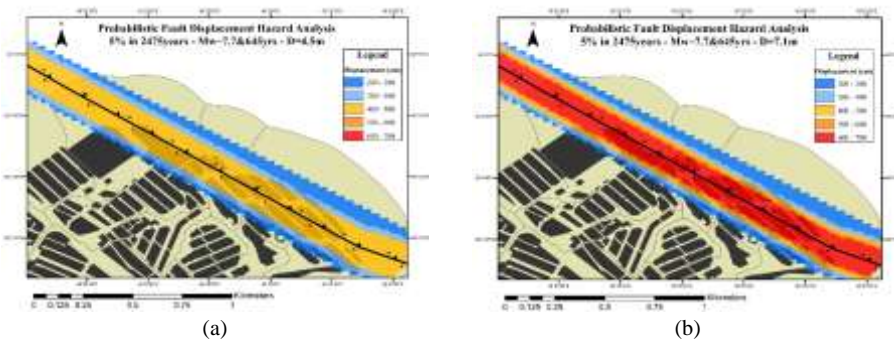
512

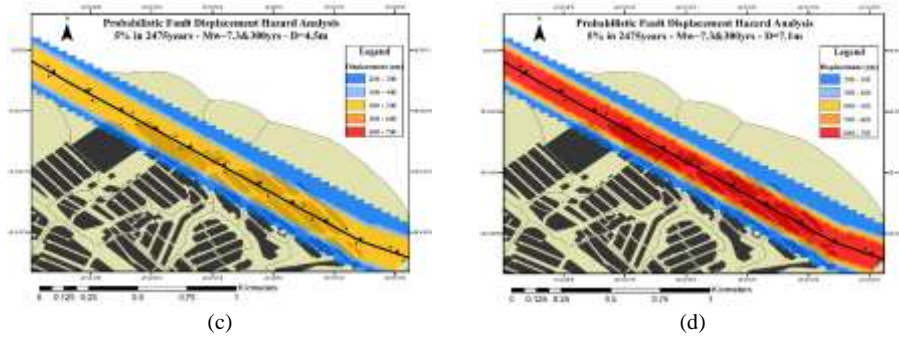
513

514

515

516





517
 518 Figure 8. Probability Displacement of 5% in 2475, a) Mw~7.7 and return period of 645yrs for D=4.5m, b) Mw~7.7 and return period of 645yrs
 519 for D=7.1m, c) Mw~7.3 and return period of 300yrs for D=4.5m and d) Mw~7.3 and return period of 300yrs for D=7.1m

520

521

Formatted: Font: (Default) Times New Roman,
 Complex Script Font: Times New Roman

522

523

524

525

526

527

528 **List of Tables:**

Formatted: Font: Bold, Complex Script Font: Bold

529

530
531
532
533
534
535

Table 1. Probability of distributed rupture for different cell sizes (Petersen et al., 2011)

No.	Cell Size (m ²)	a(z)	b(z)	Standard Deviation(σ)
1	25×25	-1.1470	2.1046	1.2508
2	50×50	-0.9000	0.9866	1.1470
3	100×100	-1.0114	2.5572	1.0917
4	150×150	-1.0934	3.5526	1.0188
5	200×200	-1.1538	4.2342	1.0177

Formatted: No underline

536
537
538
539
540
541
542
543
544

Table 2. mapping measured the mapped fault

Summary of accuracy: The distance from trace to the

observed surface rupture (Petersen et al., 2011)

Mapping Accuracy	Mean (m)	One-Sided Standard Deviation (m)	Two-Sided Standard Deviation on Fault (m)
ALL	30.64	43.14	52.92
Accurate	18.47	19.54	26.89
Approximate	25.15	35.89	43.82
Concealed	39.35	52.39	65.52
Inferred	45.12	56.99	72.69

545
546
547

Table 3. Different Models Used in Principal Fault Attenuation Relationships (Petersen et al., 2011)

Analysis Type	Model	Weight
Multivariate	BILINEAR $\ln(D)=1.7969Mw+8.5206(l/L)-10.2855, \sigma_{in} = 1.2906, l/L < 0.3$ $\ln(D)=1.7658Mw-7.8962, \sigma_{in} = 0.9624, l/L \geq 0.3$	0.34
	QUADRATIC $\ln(D)=1.7895Mw+14.4696(l/L)-20.1723(l/L)^2-10.54512, \sigma_{in} = 1.1346$	0.33
	ELLIPTICAL $\ln(D)=3.3041 \sqrt{1 - \frac{1}{0.5^2} [(l/L) - 0.5]^2} + 1.7927Mw - 11.2192, \sigma_{in} = 1.1348$	0.33

548